Construction of a MRI-based 3D Atlas of the Human Tongue for Biomechanical Tongue Modeling

Chao-Min Wu, Goh Han Tiet, Sung-Yi Wang
Department of Electrical Engineering
National Central University

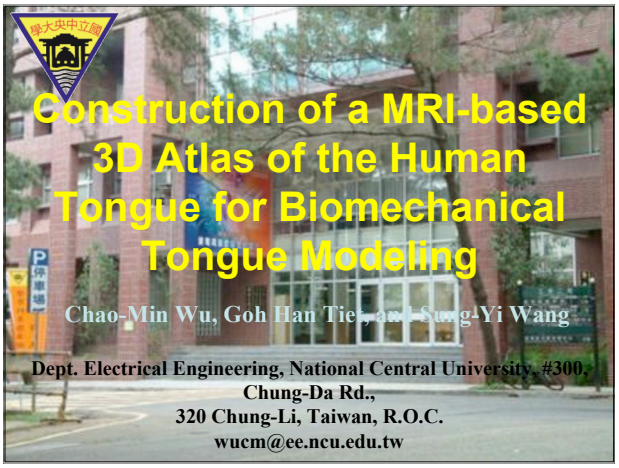

Purpose

- **The main purpose of this study is to build a MRI-based 3D tongue atlas for research on tongue morphometrics and biomechanical tongue modeling.**

Introduction

- Recently MRI related research has been moved from the study of the vocal tract configuration [1][2][3] to the internal musculature deformation of the human tongue [4][5][6].

  However, these studies were:
  - 1) single subject study [4][5][6],
  - 2) lack of statistical analysis capability [4][5], and
  - 3) with limited tongue muscles being assessed [4][5].

Introduction

- Recent studies on 3D tongue shape of either 5 speakers [7] or 1 speaker [8], however, they used MRI images for acoustic factor analysis of vowel production. Other MRI-based tongue deformation study [9] was focused on the role and deformation of human tongue in the swallowing mechanism.

Introduction

- In this study, MRI data of 8 subjects (4 males and 4 females) were chosen from an orally-based MRI database of 20 male and 20 female college students without speech disorders. The axial MR images of the human tongue were first segmented with snake active contour method, the 3D tongues of each subject were reconstructed with morphology-based grey-level interpolation.

Introduction

- **We used our MRI database to build a 3D tongue atlas for male and female subjects, respectively, with the thin-plate spline method.**

OPAL-09, June 26-27, 2009, Vancouver, BC, CA

Materials and methods

- Subjects: The subjects for the MRI data were 20 male and 20 female college students (19-28 years old) who are native speakers of mandarin with Taiwanese accent without speech disorders.

Materials and methods

- **Protocol:** The oral MR images (axial: TR, 400ms; TE, 10 ms, FOV 24 × 24; image matrix, 256 × 256 for 35 slices with 2 mm thickness) were acquired using a GE SIGNA 1.5 Tesla scanner in the university hospital of Chung Shan Medical University. The scanning area covered the levels from the line that connects the ANS (anterior nasal spine) and dens of the Axis (the second cervical vertebrae) to the bottom of the tongue (see Fig. 1a). For the purpose of future evaluation of 3D reconstruction, images of the sagittal (TR, 416ms; TE, 10 ms, FOV 24 × 24; image matrix, 256 × 256 for 20 slices with 3 mm thickness, see Fig. 1b) and coronal (TR, 400ms; TE, 10 ms, FOV 24 × 24; image matrix, 256 × 256 for 14 slices with 5 mm thickness) orientations were also acquired for each subject, respectively.

MRI Localizer

Fig. 1 (a) the Axial slices localizer; (b) the sagittal slices localizer.

Segmentation with Snake Algorithm

Fig. 2 : Upper-left : The user has pulled the initial active contour near to desired contour. Upper-righ : The snake illustrates in stabilities that may be a result. Lower-left : The edge of tongue selected by snake. Lower-righ: The tongue contour.

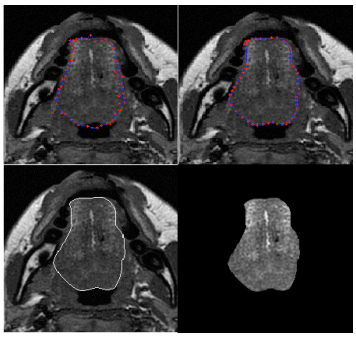

Image Processing

- The axial MR images of the human tongue were first segmented with snakes active contour method, then the 3D tongues of each subject were reconstructed with morphology-based grey-level interpolation [10], finally these 3D tongues were spatial transformed into a 3D tongue atlas with thin-plate spline method. Outline of image processing is shown in Fig. 3.

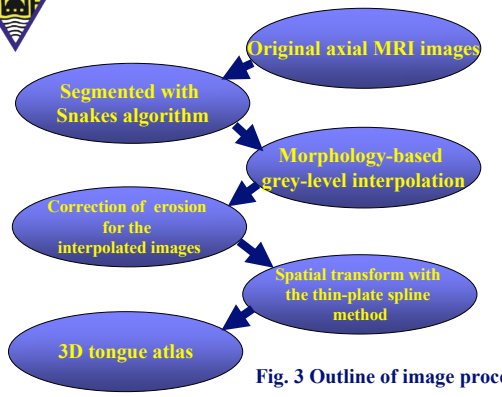

Fig. 3 Outline of image processing

Fig. 4 Reconstructed 3D tongue of the first female subject and its corresponding midsagittal slice

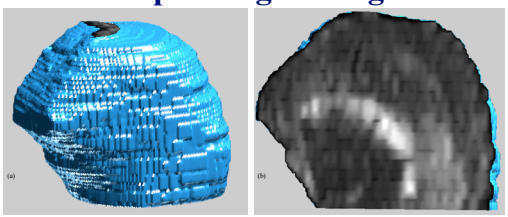

Landmark Selection

- **Landmarks:** Sixteen landmarks were defined and selected from the 3D reconstructed MRI tongue images based on the subjects.
- Landmarks are the homologous points that define locations having anatomical significance and identifiable geometric coordinates.

Landmark Selection

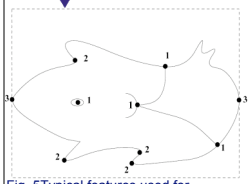

Fig. 5Typical features used for landmark selection [11] are intersection among different anatomical structures (Type 1), maxima of curvatures, and centroids of closed-boundary regions (Type 2), and extrema on a contour (Type 3), etc.

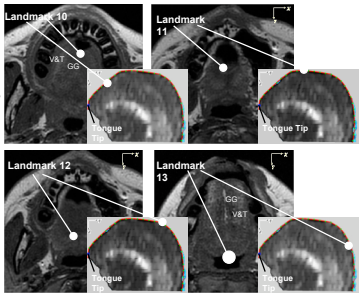

Fig. 6 Auxilliary landmark selection: landmarks were selected from a contour (red) line, on the mid-sagittal MRI slice, where equal distance (0.5mm) was segmented with points (green). Landmarks 10-13 were selected every 5 Segments as shown in white points.

Table 1. Landmarks for 3D Tongue

(Ant. Anterior; Pos. Posterior; Lat. Lateral; Dos. Dorsal; V Verticalis; T Transversus; SL Superior Longitudinalis; IL Inferior Longitudinalis; GG Genioglossus; HG Hyoglossus; SG Styloglossus muscle)

Number	Name	Type	Description
1	Ant. Tip point	3	Ant. most point on the tongue
2	SG-HG Left	1	Left SG-HG Intersection point
3	SG-HG Right	1	Right SG-HG Intersection point
4	GG-IL Left	1	Left GG-IL Intersection point
5	GG-IL Right	1	Right GG-IL Intersection point
6	SL-VT Left	1	Left SL-VT Intersection point
7	SL-VT Right	1	Right SL-VT Intersection point
8	SL-VT Ant.	1	Ant. SL-VT Intersection point
9	SL-VT Pos.	1	Pos. SL-VT Intersection point
10	Tongue Front Point	2	Midsagittal tongue surface front point
11	Tongue Center Point	2	Midsagittal tongue surface center point
12	Tongue Back Point	2	Midsagittal tongue surface back point
13	Tongue Root Point	2	Midsagittal tongue surface root point
14	Internal Left Point	2	Internal left point on the MRI slice of landmark 9
15	Internal Right Point	2	Internal right point on the MRI slice of landmark 9
16	SL-VT Bottom	2	Intersection point of SL-VT and median septum

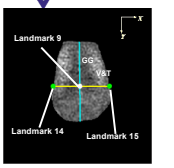

Fig. 7 Locating landmarks 14,15

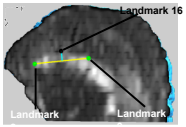

Fig. 8 Locating landmarks 16.

Thin-plate Spline Mapping

Thin-plate spline analysis (TPS) [12] was used to build a 3D tongue atlas for male and female subjects, respectively.

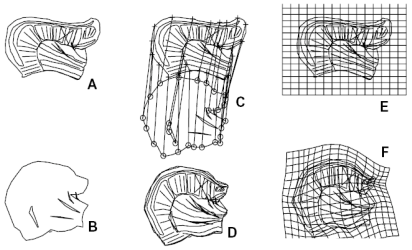

Fig. 10 Demonstration of the mapping with 2-d thin-plate splines (Handdrawn polygons were used in this example to show the concept.) **A** A typical sketch of a tongue section. **B** Outline of tongue as obtained from MRI. **C** Specification of corresponding landmarks (here landmark pairsfor **A** and **B**). **D** Panel **A** mapped onto panel **B** with thin-plate spline to make all landmarks coincide **E**-**F** Demonstration of the mapping by using a grid.

2D Thin-plate Spline Method

Mapping function

$$\Phi(P) = a_1 + a_x x + a_y y + \sum_{i=1}^{n} \omega_i U(|P - P_i|)$$

$$W = \begin{pmatrix} \omega_1 & \cdots & \omega_n & a_1 & a_x & a_y \end{pmatrix}$$

2 × (n+3) Matrix

For 3D TPS

$$U(r) = r^2 \log r^2 \qquad U(r) = |r|$$

$$r_{ij} = |P - P_i| \qquad r_{ij} = |P_i - P_j|$$

All points of Panel A in Fig. 10

Landmark i of Panel A in Fig 10

Panels A and B mapping matrix

$$L = \begin{pmatrix} K & Q \\ Q^T & 0 \end{pmatrix}$$

$$K = \begin{pmatrix} 0 & U_{12} & \cdots & U_{1n} \\ U_{21} & 0 & \cdots & U_{2n} \\ \vdots & \vdots & \ddots & \vdots \\ U_{n1} & U_{n2} & \cdots & 0 \end{pmatrix}$$

$$Q = \begin{pmatrix} 1 & x_1 & y_1 \\ 1 & x_2 & y_2 \\ \vdots & \vdots & \vdots \\ 1 & x_n & y_n \end{pmatrix}$$

Landmark i of Panel A in Fig 10

$$L \quad W = M$$

$$M = (h_1 \quad \cdots \quad h_n \quad 0 \quad 0 \quad 0)^T$$

Landmark i of Panel B in Fig 10

$$W = (\omega_1 \quad \cdots \quad \omega_n \quad a_1 \quad a_x \quad a_y)^T = L^{-1}M$$

3D Atlas of the Human Tongue

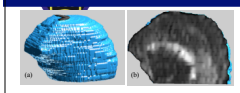

Fig 11. (a) 3D tongue of the first female subject; (b) Midsagittal section

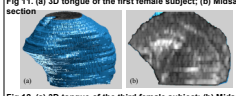

Fig 12. (a) 3D tongue of the third female subject; (b) Midsagittal section

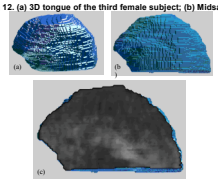

Fig. 13. 3D tongue atlas of 4 female subjects (a) 3D view; (b) side view; (c) midsagittal slice

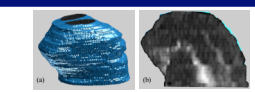

Fig. 14 (a) 3D tongue of the first male subject; (b) Midsagittal section

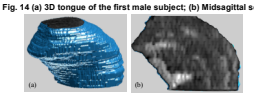

Fig. 15 (a) 3D tongue of the third male subject; (b) Midsagittal section

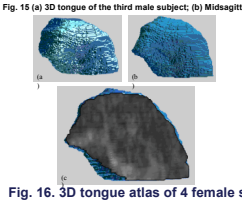

Fig. 16. 3D tongue atlas of 4 female subjects (a) 3D view; (b) side view; (c) midsagittal slice

Discussion

Sagittal sections of the original MRI data were used to evaluate the accuracy of image registration and reconstruction. The resulted 3D tongue atlas was used to study subject-to subject, subject-to-atlas, and male-to-female morphometric variation.

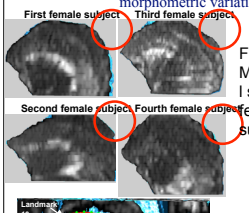

Fig 17. Midsagittal slices of female subjects

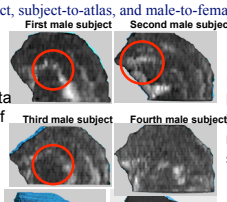

Fig 18. Midsagittal slices of male subjects

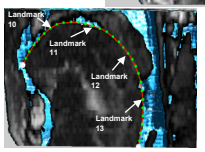

Fig 19. Redefine landmarks 10-13 with equal ratios

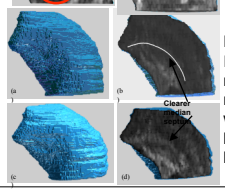

Fig 20. Improvement of mapping with new landmark locations

Summary

- **Our results show the major difference among female subjects before and after the TPS analysis is in the area of tongue dorsum that is close to the velum and epiglottis, respectively. However, the major difference among male subjects is in the areas of tongue tip and body regardless of TPS analysis. In summary, our preliminary results imply that the 3D tongue atlas of female subjects show less subject-to-subject difference.**
- **These atlases will be used as the basis for future research on biomechanical tongue modeling.**

References

- [1] Narayanan, S. S., A.A. Alwan, and K. Haker (1995) *J. Acoust. Soc. Am.*, 98: 1325-1347.
- [2] Story, B., I. Titze, and E. A. Hoffman (1996) *J. Acoust. Soc. Am.*, 100: 537-554.
- [3] Narayanan, S., D. Byrd, and A. Kaun (1999) *J. Acoust. Soc. Am.*, 106: 1993-2007.
- [4] Stone, M. et al. (2001), *J. Acoust. Soc. Am.*, 109: 2974-2982.
- [5] Takano, S. and K. Honda (2001) *Spring meeting, J. Acoust. Soc. Japan.*
- [6] Wu, Chao-Min (1996) *Ph.D. thesis*, The Ohio State University, Columbus, OH.
- [7] Zheng, Y., Hasegawa-Johnson, M., and Pizza, S. (2003) J. Acoust. Soc. Am., 113: 478-486.
- [8] Engwall, O. (2003) Speech Communication, 41: 303-329.
- [9] Napadow, V. J., Kamm, R. D., and Gilbert, R. J. (2002) J. Biomech. Eng., 124: 547-556.
- [10] G. J. Grevera and J. K. Udupa (1996) *IEEE Tran. Med. Img.* 15: 881-892.
- [11] Bookstein, F.L. (1991) Morphometric tools for landmark data. Cambridge: Cambridge University Press, pp. 55–87.
- [12] Bookstein, F. L. (1989) "Principal Warps:Thin-Plate Splines and the Decomposition of Deformations," IEEE Transactions on Pattern Analysis and Machine Intelligence, Volume 11, Issue 6, pp. 567 – 585.